Journal of Materials Chemistry A

PAPER

View Article Online
View Journal | View Issue

Cite this: J. Mater. Chem. A, 2014, 2, 7229

A high performance electrochemical sensor for acetaminophen based on a rGO–PEDOT nanotube composite modified electrode†

Tzu-Yen Huang,[ab] Chung-Wei Kung,[a] Hung-Yu Wei,[bc] Karunakara Moorthy Boopathi,[be] Chih-Wei Chu*[bd] and Kuo-Chuan Ho*[ac]

Received 19th January 2014
Accepted 25th February 2014

DOI: 10.1039/c4ta00309h

www.rsc.org/MaterialsA

In this study, we perform an electrochemical sensing using a conductive composite film containing reduced graphene oxide (rGO) and poly(3,4-ethylenedioxythiophene) nanotubes (PEDOT NTs) as an electrode modifier on a glassy carbon electrode (GCE). Scanning electron microscopy suggests that the rGO covers the surface of GCE uniformly and the PEDOT NTs act as a conducting bridge to connect the isolated rGO sheets. By combining these two materials, the conductivity and the surface coverage of the film can be enhanced, which is beneficial for electrochemical sensing. The rGO–PEDOT NT composite modified electrode is applied for an effective sensor to analyze acetaminophen. The obtained electrochemical activity is much higher than those obtained by the rGO- and PEDOT NT-modified electrodes; the higher electrochemical activity may be attributed to the higher conductivity and greater coverage of the rGO–PEDOT NT composite film on the GCE. Furthermore, interference tests indicate that the rGO–PEDOT NT composite modified electrode exhibits high selectivity toward the analyte. This novel method for combining the rGO and PEDOT NTs establishes a new class of carbon material-based electrodes for electrochemical sensors.

1 Introduction

Acetaminophen (*N*-acetyl-*P*-aminophenol or paracetamol) is one of the most extensively used drugs in the world; it is mainly used to reduce fever and relieve headache, backache, arthritis, postoperative pain and so on.[1,2] Overdoses of acetaminophen produce accumulation of toxic metabolites, which may cause severe and sometimes fatal hepatotoxicity and nephrotoxicity.[3] Thus, developing accurate analytical techniques such as effective sensors for detecting acetaminophen becomes an important issue. Some analytical methods, such as spectrophotometry,[4] liquid chromatography,[5] titrimetry,[6] capillary electrophoresis,[7] chemiluminescence[8] and electrochemical methods,[9–11] have been applied for the determination of acetaminophen. Compared to other analytical approaches, electrochemical methods show the advantages of short response time, simplicity, low cost, high sensitivity, and high selectivity toward the analyte.

Graphene oxide (GO) consists of a single atomic layer of sp^2-bonded carbon atoms functionalized with mainly phenol, hydroxyl, and epoxide groups on the basal plane and ionizable carboxyl groups at the edges; it is obtained after treating graphite with strong oxidizers. With extraordinary electronic transport property and high electrocatalytic activity, GO has been widely used as the electrode material in several fields of applications.[12–16] In general, the unique properties of GO such as good mechanical strength, large specific surface area, and high conductivity have attracted great attention in developing GO as electrochemical sensors.[17–20]

Poly(3,4-ethylenedioxythiophene) (PEDOT) is a conducting polymer which has been investigated in several areas of application, including solar cells,[21,22] electrochromic devices,[23,24] and electrochemical sensors.[25–30] Due to its excellent electrocatalytic activity, PEDOT was applied as an electrochemical sensor for nitrite,[25–27] iodate,[28] hydrogen peroxide,[29] and acetaminophen.[30] Recently, some nanostructures of PEDOT, including nanorods,[26,27] nanospheres,[29,31] and nanoflowers,[32] have been developed in order to further enhance the electrocatalytic activity of PEDOT. Compared to these nanostructures, one-dimensional (1D) nanotubes are known for their advantages of facile electron transportation and the relatively larger surface area compared to the nanorods or nanowires. Thus, PEDOT nanotubes have been applied for dye-sensitized solar cells[33] and electrochromic

[a]Department of Chemical Engineering, National Taiwan University, Taipei 10617, Taiwan. E-mail: kcho@ntu.edu.tw; Fax: +886-2-2362-3040; Tel: +886-2-2366-0739
[b]Research Center for Applied Sciences, Academia Sinica, Taipei 11529, Taiwan. E-mail: gchu@gate.sinica.edu.tw; Fax: +886-2-2782-6680; Tel: +886-2-2789-8000 ext. 270
[c]Institute of Polymer Science and Engineering, National Taiwan University, Taipei 10617, Taiwan
[d]Department of Photonics, National Chiao-Tung University, Hsinchu 30010, Taiwan
[e]Department of Engineering and System Science, National Tsing Hua University, Hsinchu 30010, Taiwan

† Electronic supplementary information (ESI) available. See DOI: 10.1039/c4ta00309h

devices[34] in order to enhance the performance of these devices. However, to the best of our knowledge, PEDOT nanotubes have not been used for the detection of acetaminophen.

In the field of electrochemistry, carbon nanomaterials have been used as modifiers in a modified electrode.[35,36] Among several carbon nanomaterials, graphene has been confirmed to be an excellent modifier in electrochemical applications.[37–39] Since nanocomposites or nanohybrids can combine the advantages of each component and exhibit enhanced properties,[40–42] combining other carbon materials with graphene becomes a strategy to further enhance the electrocatalytic activity of the graphene-based modified electrodes. For example, carbon nanotubes (CNTs) and graphene show similar conducting properties, but the drawbacks of each material limit themselves for application in an electrochemical field.[37,43] Combining the 1D CNTs with the two-dimensional (2D) graphene became an approach to achieve a better performance for electrochemical applications.[44] Thus, the nanocomposites or nanohybrids of 2D graphene and 1D electrocatalytic materials, such as nanotubes or nanowires, are expected to show an enhanced electrocatalytic property.

In this study, we prepared rGO–PEDOT nanotube composites as modifiers on glassy carbon electrodes (GCEs) for the electrochemical detection of acetaminophen. To the best of our knowledge, this is the first report to integrate the advantages of 1D nanotubes of PEDOT and 2D graphene and apply the composite for electrochemical applications. We attempt to use PEDOT nanotubes for acetaminophen sensing. The film of rGO–PEDOT nanotubes exhibited much better electrocatalytic activity toward the analyte compared to those of its individual constituents. The noncovalent preparation of rGO–PEDOT nanotubes provides the high conducting properties of the obtained composite, resulting in better electrocatalytic properties; it brings attractive interest for the development of nanocarbon materials with potentially improved conductivity and catalytic ability for electrochemical research.

2 Experimental

2.1 Chemicals

Graphite powder (Bay Carbon Inc. (USA), SP-1), poly(3,4-ethylenedioxythiophene) nanotubes (PEDOT NTs), acetaminophen (AP), glucose (Glu), nitrite (Nit), methanol (MeOH) and ethanol (EtOH) were purchased from Sigma-Aldrich. All other chemicals were of analytical grade and used without further purification. Aqueous solutions were prepared using doubly distilled water. The supporting electrolyte for the electrochemical studies was 0.1 M phosphate buffer solution (PBS, pH 7), which was prepared from Na_2HPO_4 and NaH_2PO_4 solutions. All solutions were deoxygenated by purging with pre-purified N_2 gas.

2.2 Apparatus & measurement

Cyclic voltammetry (CV) and differential pulse voltammetry (DPV) was performed using a CHI 440 analytical system (CH Instruments) and its compatible software. A conventional three-electrode cell assembly, consisting of an Ag/AgCl reference electrode and a Pt wire counter electrode, was used for the electrochemical measurements. The working electrode was either an unmodified GCE or a GCE modified with materials (exposed area = 0.070 cm^2). Additionally, the GCEs modified with materials was measured in 10 mM $K_3[Fe(CN)_6]$ with 0.1 M KCl solution to obtain the CV curves and calculate for the electrochemically active surface area. All measurements were performed at 25 ± 2 °C. The surface morphologies of the composites were investigated using scanning electron microscopy (SEM, Hitachi S-4700). The PEDOT NT solution was dropped on a holey carbon-coated copper grid (Lacey Carbon Type-A 300 mesh copper grid; TED Pella) and then dried in air at 70 °C prior to characterization using TEM (JEM 2100F). An alpha 300 Raman spectrometer (WITec Instruments, Germany) was used to analyze the compositions of the composite films with a fixed wavelength of 514.5 nm. The XPS spectra were recorded using a PHI 5000 VersaProbe (ULVAC-PHI, Chigasaki, Japan) system with He(I) ($h\nu$ = 21.2 eV) as the energy source. X-ray diffraction spectra analysis was conducted for phase identifications by using a powder X-ray diffractometer (XRD; X'Pert PRO-PANalytical, CuKα radiation).

2.3 Preparation of the rGO–PEDOT NT-modified electrode

GO was prepared from graphite powder using a modified version of the Hummers' method.[45] Briefly, graphite powder (2 g), $NaNO_3$ (1 g), and H_2SO_4 (46 mL) were mixed in an ice bath and then $KMnO_4$ (6 g) was added slowly. Once mixed, the solution was transferred to a water bath and stirred at 35 °C for approximately 1 h, forming a thick paste. Water (80 mL) was added and then the solution was stirred for 1 h at 90 °C. Finally, more water (200 mL) was added, followed by the slow addition of H_2O_2 (30%, 6 mL). The warm solution was filtered and washed sequentially with 10% HCl (3 × 200 mL) and water (200 mL). The filter cake was dispersed in water through mechanical agitation and then stirred overnight. The dispersion was left to settle and the supernatant (clear yellow dispersion) was subjected to dialysis for 1 month, resulting in a stock solution having a GO concentration of approximately 0.17 mg mL^{-1}. The stable dispersion was filtered through an alumina membrane and left to dry for several days. The GO paper was then carefully peeled from the filter and stored under ambient conditions. To produce a hybrid suspension of rGO and PEDOT NTs, dry powders of GO and PEDOT NTs were dispersed directly in anhydrous hydrazine and stirred for 24 hours. Hydrazine bubbled violently upon contact with the powders of GO and PEDOT NTs, but soon formed a uniform dark gray suspension with no visible precipitation. After mixing the materials with hydrazine solution, the dark gray suspension was centrifuged to separate out the residual bundles of PEDOT NTs and aggregated rGO. After centrifugation, the uniformity of the rGO–PEDOT NT dispersion was ensured through heating at 60 °C with repeated ultrasonic agitation for approximately 30 min. Typically, a mixture of GO (1 mg mL^{-1}) and PEDOT NTs (3 mg mL^{-1}) in hydrazine was employed to prepare a modified electrode.

Bare GCEs were used for modification. Before starting each experiment, GCEs were polished using a BAS polishing kit and a

slurry of 0.05 μm aluminium oxide (Al_2O_3) powder and then rinsed sequentially with deionized water and ethanol. The GCEs were coated uniformly with the dispersion of rGO–PEDOT NTs (4 μL) and dried in an oven. The obtained rGO–PEDOT NT-modified GCEs were washed carefully in deionized water to remove residual materials and solvent from the GCE, and then dried at room temperature.

3 Results and discussions

3.1 Characterization of the rGO–PEDOT NT composite film

The crystal structures of the GO, rGO, PEDOT NTs and rGO–PEDOT NTs were first characterized by XRD (Fig. 1(a)). The graphite materials were treated by oxidation and exfoliation. The diffraction peak of GO appears at 11.3°, indicating an estimated interlay space of 0.78 nm; this value is similar to that reported in the literature.[46,47] This interlay space is attributed to the introduction of oxygenated functional groups on carbon sheets. On the other hand, the diffraction peak disappeared after the subsequent reduction, which confirms the significant reduction of oxygenated groups and the high exfoliating degree of the layered graphene.[48] The weak diffraction of PEDOT NTs locates at a 2θ value of ~25°, which is a characteristic of amorphous polymeric materials.[49] The composite material reveals the property from rGO and PEDOT NTs, which is worth to be further investigated by Raman spectroscopy and X-ray photoelectron spectroscopy (XPS).

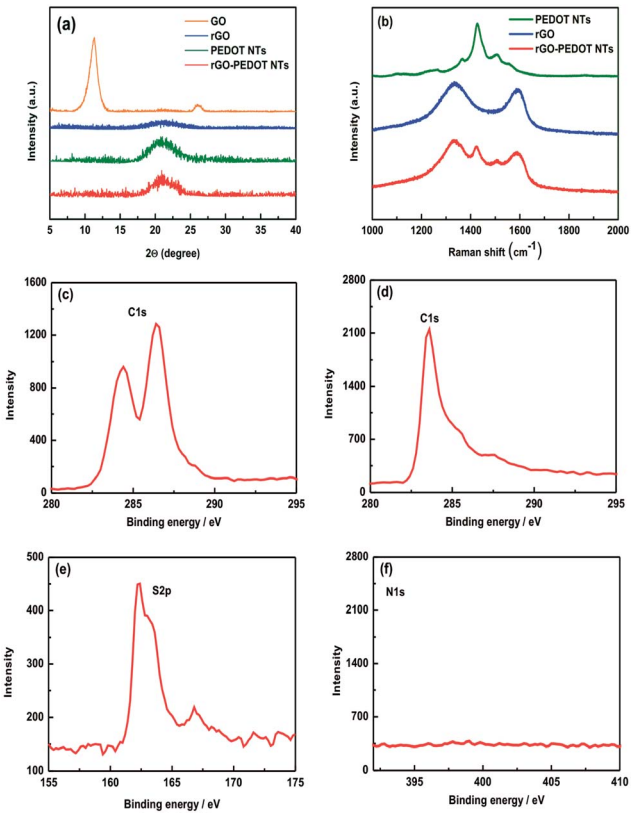

Fig. 1 (a) and (b) The XRD pattern and Raman spectra of GO, rGO, PEDOT NTs and rGO-PEDOT NTs. The XPS spectra of the composite material before and after reduction. (c) and (d) The C1s of rGO–PEDOT NTs as-prepared and after reduction of the rGO–PEDOT NT composite. (e) The S2p of rGO–PEDOT NT composite. (f) shows no residual solvent to prevent the interference.

Fig. 1(b) shows the Raman spectra of PEDOT NTs, rGO and rGO–PEDOT NT composites. PEDOT NTs show two strong bands at 1428 and 1506 cm^{-1}, which are attributed to the symmetric stretching mode and asymmetric stretching vibration of the –C=C– bond in PEDOT, respectively.[50] The 1365 and 1267 cm^{-1} bands are attributed to the stretching modes of single C_α–$C_{\alpha'}$ bonds and the C_α–$C_{\alpha'}$ inter-ring bonds.[51] The rGO exhibits two strong bands located at 1335 and 1590 cm^{-1}, attributed to the D band arising from the breathing mode of κ-point photons of A_{1g} symmetry and the G band represents the E_{2g} phonon of sp^2 C atoms in the graphene network.[52] It is clearly seen that rGO–PEDOT NT composites possess the property of PEDOT NTs and rGO simultaneously; the hybrid film retains the signal at 1423 and 1509 cm^{-1} from PEDOT NTs and the signal at 1333 and 1589 cm^{-1} from the rGO, indicating that the PEDOT NTs and rGO co-existed and maintained their individual electronic properties.

We also performed XPS measurements on the rGO–PEDOT NT composite before and after reduction to evaluate the removal of oxygen containing groups. The C1s XPS spectrum of the as-prepared GO–PEDOT NT composite (Fig. 1(c)) clearly shows a considerable oxygen content and carbon atoms with functional groups: the carbon in C–O bonds (hydroxyl and epoxy, 286.4 eV) and the nonoxygenated ring carbon (C–C, 284.6 eV). After reduction, the C1s XPS spectrum becomes a single symmetrical peak at 284.4 eV (Fig. 1(d)), indicating that the composite is successfully reduced by hydrazine solution. Besides, the signal (162.2 eV) from the S2p XPS spectrum of the rGO–PEDOT NT composite retains the intensity, indicating that the chemical reduction for the composite does not affect the property of the PEDOT NTs (Fig. 1(e)). No signals appear in the N1s XPS spectrum of the rGO–PEDOT NT composite (Fig. 1(f)); this observation clarifies that the hydrazine solution is fully removed after preparing the composite, which eliminates the interference issue for practical biomedical applications.

Fig. 2 shows the scanning electron microscopy (SEM) images of the PEDOT NTs and rGO–PEDOT NT composite material. The hollow feature of one PEDOT NT can be clearly observed in the TEM image shown in the inset of Fig. 2(a). Heavily entangled bundles of PEDOT NTs can be observed on the film of the pristine PEDOT NTs (Fig. 2(a)), resulting in a non-uniform coverage of the PEDOT film across the surface of the substrate. This observation implies that the PEDOT NT modified electrode may lead to the inferior electrochemical background because of its poor surface coverage.

The SEM images of the rGO–PEDOT NT composite film are shown in Fig. 2(c). It can be seen that the PEDOT NTs are adhered on top and bottom of the rGO sheets and combine the unique 2D conducting properties of rGO to form the higher conducting composite. Compared to the poor coverage of PEDOT NTs on the substrate, Fig. 2(b) shows that the 2D rGO sheets can provide a superior coverage on the substrate, but they also suffer from poor electron conduction between the

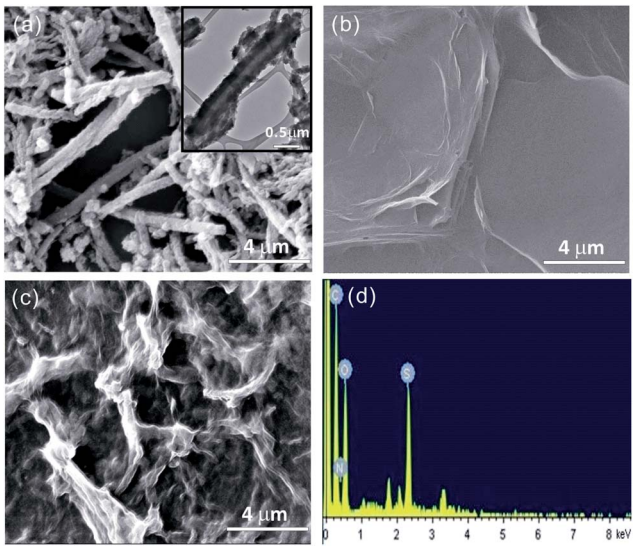

Fig. 2 SEM images of (a) pristine PEDOT NTs, (b) rGO and (c) rGO–PEDOT NT composite; (d) EDS of the rGO–PEDOT NT composite film. The inset in (a) shows the TEM image for the hollow feature of one PEDOT NT.

isolated rGO regions. The PEDOT NTs can act as conductive bridges to connect the isolated rGO regions and minimize the barrier for electron transfer between those rGO sheets. On the other hand, rGO sheets act as a blanket in the composite film to cover all the PEDOT NTs and smoothen the surface of the film. Thus, blending the rGO and PEDOT NTs does combine their own unique advantages and turns the nanocomposite into a preferable material. The energy dispersive spectrum (EDS) of the rGO–PEDOT NT composite film is shown in Fig. 2(d). The significant signals of C, O, and S, which are the elements present in rGO and PEDOT, can be observed in Fig. 2(d). The signal of N in Fig. 2(d) is neglectable, indicating that the hydrazine has been removed.

3.2 Electrochemical behavior of the rGO–PEDOT NT modified electrode

Cyclic voltammetry (CV) was used to investigate the electrochemical behavior of a bare GCE and the electrodes modified with rGO, PEDOT NTs, and rGO–PEDOT NT composite, recording at a scan rate of 100 mV s^{-1} in N_2-saturated PBS; these CV curves are shown in Fig. 3(a). From Fig. 3(a), it can be observed that the unmodified (bare) GCE exhibited no obvious redox peaks in PBS at the applied potentials between −0.6 and +0.6 V. On the other hand, the modified electrodes of PEDOT NTs and rGO showed redox peaks, with the formal potentials of −8 and 38 mV, respectively. The rGO–PEDOT NT modified electrode also exhibited a well-defined redox couple with a formal potential of −18 mV; it was attributed to the coupling of the electrochemical properties contributed from both the rGO and the PEDOT NTs. Although the rGO exhibited excellent 2D conducting properties, the gaps between isolated rGO layers impeded charge transfer, resulting in the formation of a barrier. From CV traces, it can be seen that the background current of

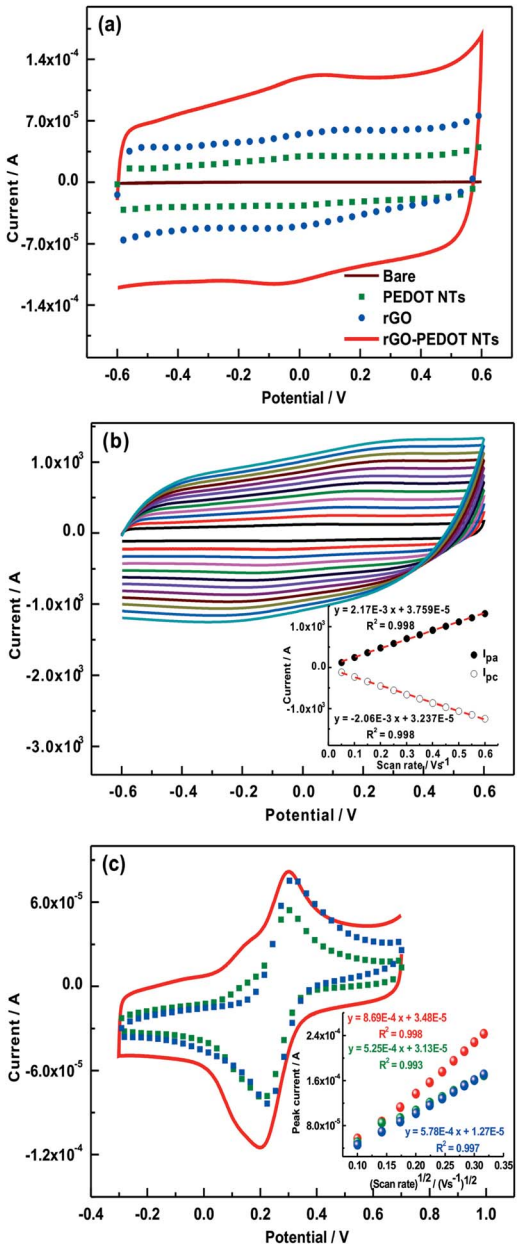

Fig. 3 (a) CV curves of the bare GCE and GCEs modified with PEDOT NTs, rGO, and rGO–PEDOT NT composite films in N_2-saturated PBS (pH 7.0); potential scan between +0.6 and −0.6 V; scan rate: 0.030 V s^{-1}. (b) CV curves of the GCE modified with the rGO–PEDOT NT composite film in N_2-saturated PBS at scan rates (from inner to outer) of 0.05, 0.10, 0.15, 0.20, 0.25, 0.30, 0.35, 0.40, 0.45, 0.50, 0.55, and 0.60 V s^{-1}. Inset: peak currents (I_{pa} and I_{pc}) plotted with respect to the scan rate. (c) CV curves obtained from GCEs modified with PEDOT NTs, rGO, and rGO–PEDOT NT composite films in 10 mM $K_3[Fe(CN)_6]$ with 0.1 M KCl as the supporting electrolyte.

the rGO modified electrode is larger than that of the unmodified GCE, but it is still much lower than that of the composite modified electrode due to those isolated rGO regions. As for the PEDOT NT modified electrode, its unique property for one-dimensional electron transfer results in a larger background current than that of the unmodified GCE, but the poor coverage on the electrode surface becomes a main disadvantage to cause

the smaller background current compared to those of the modified electrodes of rGO and rGO–PEDOT NT composites. Despite this these two special materials have their own defects, which can be solved by blending the rGO and the PEDOT NTs. The PEDOT NTs act as conductive bridges to connect the isolated rGO regions, resulting in the increased conductivity; the rGO plays the role of a blanket to enhance the coverage on the electrode surface and enhance the 2D conducting properties for the hybrid material. Thus, the rGO–PEDOT NT modified electrode can exhibit high conductivity and high current in the CV curve, which may be beneficial for sensor applications. Fig. 3(b) shows the effect of the scan rate on the electrochemical behavior of the rGO–PEDOT NT modified electrode obtained in N_2-saturated PBS. It can be seen that the rGO–PEDOT NT modified electrode exhibited high stability with an increasing scan rate. The plot of the anodic peak current (I_{pa}) and cathodic peak current (I_{pc}) with respect to the scan rate is shown in the inset of Fig. 2(b). The linear dependence ($R^2 = 0.998$ for both I_{pa} and I_{pc}) and an I_{pa}/I_{pc} ratio of close to unity can be observed between 50 and 600 mV s^{-1}, which is consistent with a reversible electron transfer process. The peak currents of the redox couples are directly proportional to the scan rate, indicating that the redox process occurring at the rGO–PEDOT NT modified electrode was a surface-confined process.

To further investigate the advantage of the rGO blending with PEDOT NTs, we performed measurements of the rGO, PEDOT NTs and rGO–PEDOT NT modified electrodes in 10.0 mM $K_3[Fe(CN)_6]$ with 0.1 M KCl solution and estimated the electrochemically active surface area from the CV traces.

The electrochemically active surface area can be estimated from the peak current by using the Randle–Sevcik equation:[53]

$$I_p = 2.69 \times 10^5 A D^{1/2} n^{3/2} \nu^{1/2} C \quad (1)$$

where n is the number of electrons involved in the redox reaction, A is the surface area of the electrode (cm^2), D is the diffusion coefficient of the molecule in the bulk solution (6.67×10^{-6} cm^2 s^{-1} for ferricyanide[54]), C is the concentration of the molecule in the bulk solution (M), and ν is the scan rate (V s^{-1}).

Fig. 3(c) shows the CV traces of rGO, PEDOT NTs and rGO–PEDOT NT modified electrodes in 10.0 mM $K_3[Fe(CN)_6]$ with 0.1 M KCl solution. It can be observed that a higher current was obtained from the rGO–PEDOT NT composite, suggesting the superior conductivity of the composite film, thus favorable for the sensing applications. The plot of the peak current (I_{pc}) with respect to the square root of the scan rate is shown in the inset of Fig. 3(c). From the linear regression equations of rGO and PEDOT NT modified electrodes, the electrochemically active surface areas of rGO and PEDOT NT modified electrodes are calculated to be 0.083 and 0.075 cm^2, respectively, which are just slightly higher than the geometric surface area of the bare GCE (0.070 cm^2). Although the PEDOT NT modified electrode shows a highly porous feature (Fig. 2(a)), its electrochemically active surface is still quite limited. However, after blending rGO with PEDOT NTs, the electrochemical surface area reached about 0.125 cm^2, which indicates that rGO could effectively improve the poor coverage of PEDOT NTs and creates a larger surface area for the composite modified electrode. In addition, the larger electrochemical surface active area not only is useful for enhancing the sensor sensitivity, but also is beneficial for lowering the detection limit.

To further characterize the rGO–PEDOT NT modified electrode, the effect of pH on the CV traces was investigated. The CV curves of the rGO–PEDOT NT modified electrode measured in aqueous buffer solutions with various values of pH are shown in Fig. 4. The film was highly stable in the range between pH 1 and 13 and showed an obvious redox couple in each solution; this observation implies the possibility of using the rGO–PEDOT NT modified electrode for pH sensing. In particular, the CV trace recorded under the neutral conditions revealed a stable signal and a well-defined redox couple, suggesting that the system under neutral conditions would be beneficial for electrochemical sensing. The values of the anodic peak potential (E_{pa}) and cathodic peak potential (E_{pc}) were dependent on the pH of the buffer solution. The inset of Fig. 4 shows the formal potential of the rGO–PEDOT NT modified electrode with respect to the pH over the range from 1 to 13. The slope was calculated to be 61 mV pH^{-1}, which is close to the theoretical value of 59 mV pH^{-1} from the Nernst equation for an equal number of proton and electron transfer process.

3.3 Electrochemical detection of acetaminophen by the rGO–PEDOT NT modified electrode

Acetaminophen (AP), commonly known as paracetamol, is a widely used analgesic and antipyretic medicine.[55] The overdoses of acetaminophen have been found to cause fatal hepatotoxicity and nephrotoxicity, so the detection of acetaminophen becomes an important issue. Acetaminophen contains a phenolic hydroxyl group, which is electrochemically active and can be oxidized; it implies that the electrochemical detection of acetaminophen is possible.[56] The CV technique was used to investigate the electrocatalytic oxidation of acetaminophen on various electrodes which were modified with individual and

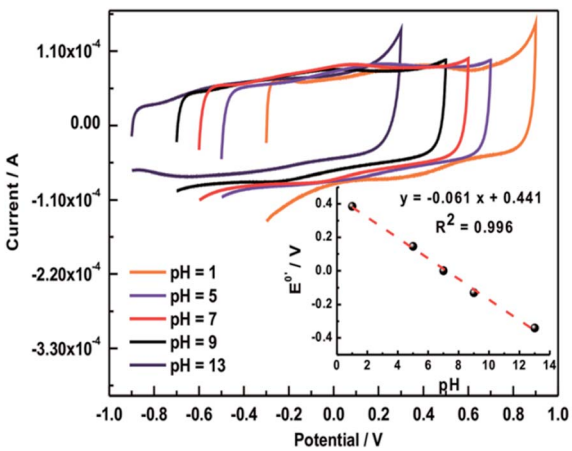

Fig. 4 CV curves of the rGO–PEDOT NT modified electrode measured in the aqueous buffer solutions with various values of pH; scan rate: 0.03 V s^{-1}. Inset: formal potential plotted with respect to the pH (1–13).

rGO–PEDOT NT composite films up to the analyte concentration of 8 mM; the CV curves are shown in Fig. 5(a). Although the peak potentials for the oxidation of acetaminophen on the PEDOT NT modified electrode and the rGO–PEDOT NT modified electrode are nearly the same, it can be noticed that the catalytic peak current for the oxidation of acetaminophen at the rGO–PEDOT NT composite film is much greater than those of the corresponding individual films. This result indicates that the combination of these two materials is not only integrating their own advantages to make the composite film more conductive, but also increasing the sensing ability toward the analyte.

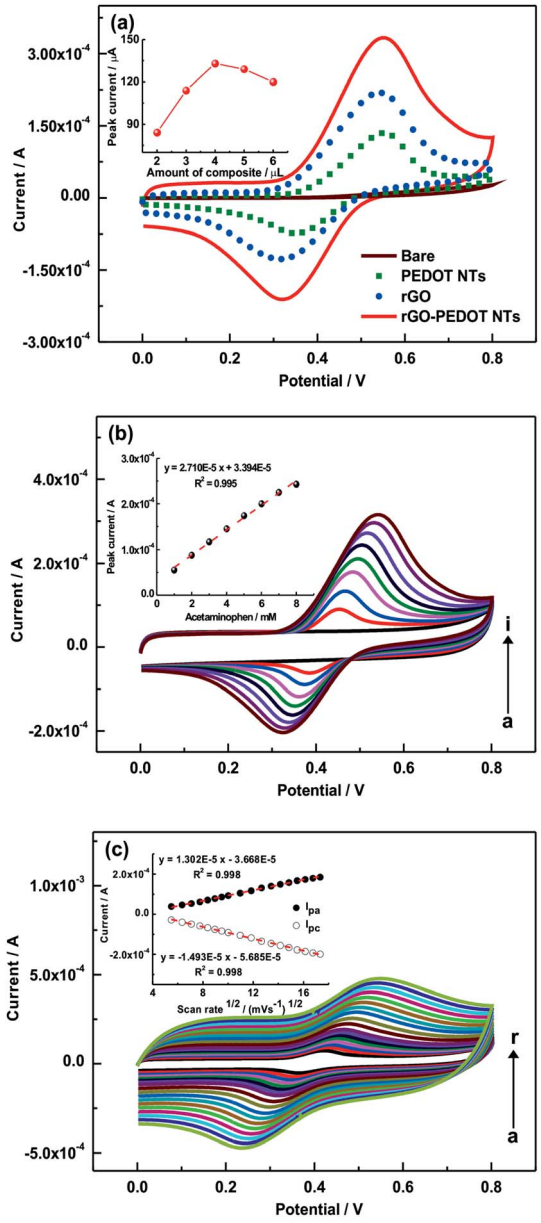

Fig. 5 (a) CV curves of a bare GCE and GCEs modified with PEDOT NTs, rGO, and rGO–PEDOT NT composite films in PBS (pH 7.0) containing 8mM acetaminophen; scan rate: 0.050 V s^{-1}. The inset shows the optimized loading amount of the rGO–PEDOT NT composite for acetaminophen detection. (b) CV curves of GCE modified with the rGO–PEDOT NT composite film with various concentrations of acetaminophen (1–8 mM); scan rate: 0.050 V s^{-1}. (c) CV curves of 0.5 mM acetaminophen at various scan rates (30–300 mV s^{-1}) (a–r). The inset shows the plot of I_{pa} and I_{pc} *versus* the square root of the scan rate.

Besides, the optimized loading amount of the rGO–PEDOT NT modified electrode was investigated in 3 mM AP solution. When the loading amount of rGO–PEDOT NTs was increased, the peak current increased until 4 μL of suspension was used. The peak current decreased when a larger amount of the composite was deposited, probably because the thicker rGO–PEDOT NT composites would cause higher resistance and lower the conductivity. Therefore, 4 μL was selected as the proper amount of modification.

The CV curves of the rGO–PEDOT NT modified electrode measured in the PBS (pH 7.0) containing various concentrations of acetaminophen are shown in Fig. 5(b). It can be observed that the catalytic current increased linearly with the increasing concentration of the analyte from 1.0 mM to 8.0 mM (R^2 = 0.995). Moreover, the anodic peak current for acetaminophen detection is 1.5 fold more than that of the reduction peak current, expressing that the composite modified electrode possesses a higher electrocatalytic activity towards the oxidation process than the reduction process.

The effect of scan rate for the detection of acetaminophen on the rGO–PEDOT NT modified electrode was recorded by CV. Fig. 5(c) shows the CV curves of the rGO–PEDOT NT modified electrode measured in 0.1 M PBS (pH 7.0) containing 0.5 mM acetaminophen at various scan rates from 30 to 300 mV s^{-1}. It can be seen that the peak currents for the redox reaction of acetaminophen increase with the increasing scan rate. Both the I_{pa} and I_{pc} are linearly related with the square root of the scan rate in the range of 30–300 mV s^{-1}, with the linear regression equations as: $I_{pa}(A) = 1.302 \times 10^{-5}\nu^{1/2}$ (mV s^{-1})$^{1/2}$ − 3.668 × 10^{-5} (R^2 = 0.998) and $I_{pc}(A) = -1.493 \times 10^{-5}\nu^{1/2}$ (mV s^{-1})$^{1/2}$ − 5.685 × 10^{-5} (R^2 = 0.998), respectively. However, the value of R^2 only gives 0.979 for the plot of I_{pa} and I_{pc} *versus* scan rate. This result indicates that the process is predominantly diffusion-controlled. A similar electrochemical behavior has been also reported in the literature using multi-walled CNT–alumina-coated silica nanocomposite modified electrodes[57] and single-walled CNT–graphene nanosheet hybrid films.[58]

The electrochemical detection of acetaminophen at the rGO–PEDOT NT modified electrode was further studied by the differential pulse voltammetry (DPV) technique. Fig. 6(a) shows the DPV responses of the rGO–PEDOT NT modified electrode in 0.1 M PBS (pH 7.0) towards various concentrations of acetaminophen. The catalytic peak current for the oxidation of acetaminophen increased linearly with increasing concentration of acetaminophen. As shown in the inset of Fig. 6(a), the rGO–PEDOT NT modified electrode achieves a sensitivity of 16.85 μA μM^{-1} cm^{-2} and a linear range from 1.0 μM to 35.0 μM (R^2 = 0.996) for the detection of acetaminophen at an applied potential of 0.38 V *vs.* Ag/AgCl/KCl (sat'd). The detection limit (S/N = 3) was estimated to be 0.4 μM. The rGO–PEDOT NT modified electrode shows a high sensitivity and excellent linearity even for the region of low analyte concentrations, which is a desirable feature for effective electrochemical sensors.

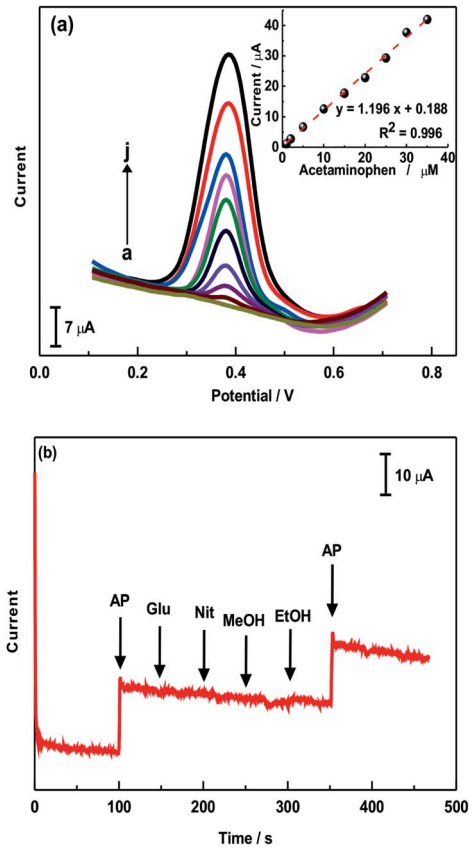

Fig. 6 (a) DPV curves of the GCE modified with rGO–PEDOT NT composite film in PBS (pH 7.0) containing various concentrations of acetaminophen (1, 2, 5, 10, 15, 20, 25, 30, and 35 μM). Inset: linear dependence of the peak current with respect to the concentration of acetaminophen. (b) Amperometric response of the rGO–PEDOT NT composite film in stirred PBS (pH 7.0), with the injections of AP, Glu, Nit, MeOH, and EtOH successively.

3.4 Interference test

The potentiostatic interference test of the rGO–PEDOT NT modified electrode for the detection of acetaminophen was examined. The applied potential was set at 0.38 V with an electrode rotation speed of 1200 rpm. The amperometric response of the rGO–PEDOT NT modified electrode was measured as a blank for the initial period of 100 s. After injecting 0.05 M acetaminophen (AP) at 100 s, various interferents including 0.5 M glucose (Glu), 0.5 M nitrite (Nit), 0.1 M methanol (MeOH), and 0.1 M ethanol (EtOH), were injected into the solution successively. The amperometric response is shown in Fig. 6(b). It can be seen that the current responses for all interferents are less than ~5%. It is also important to note that acetaminophen was added to the solution after all additions of those interferents. The modified electrode still showed a high catalytic ability toward acetaminophen after the additions of all interferents, indicating that the rGO–PEDOT NT modified electrode has excellent sensing ability to acetaminophen under the conditions with interferents and high selectivity toward the analyte.

The rGO–PEDOT NT modified electrode is compared with the acetaminophen sensors using various modified electrodes reported in the literature, and the comparison is shown in Table 1. The rGO–PEDOT NT modified electrode shows a comparable low detection limit (0.4 μM) in neutral buffer solution (pH 7.0) at a lower applied potential (0.38 V). Such features are important for the determination of acetaminophen in biological fluids during medical control. More importantly, the rGO–PEDOT NT modified electrode could retain both the wide linear range (1–35 μM) and the low detection limit (0.4 μM). In the literature, although few modified electrodes showed low detection limits, their linear ranges were relatively narrow. For example, the graphene modified electrode,[10] the graphite oxide modified electrode[56] and the SWCNT–dicetyl phosphate film modified electrode[59] showed the lower detection limits of 0.04 μM, 0.032 μM, and 0.04 μM, respectively for the electrochemical determination of acetaminophen, but their linear detection ranges were relatively narrow (0.165–26.5 μM, 0.1–20 μM, and 0.1–20 μM, respectively). Besides, the pH values of the graphene and graphite oxide modified electrodes for the detection of acetaminophen are 2.0 and 9.3, at the applied potential of about 0.61 and 0.25 V, respectively. Compared to other carbon composite modified electrodes,[57] the rGO–PEDOT NT modified electrode proposed in this study achieves a better linear detection range under biological pH conditions at a

Table 1 Comparison of acetaminophen detection for the reported electrochemical sensors

Working electrode	pH used	Linear range (μM)	Detection of limit (μM)	Applied potential (V)	Reference
rGO–PEDOT NT/GCE	7.0	1–35	0.4	0.38	This work
Graphene/GCE	9.3	0.1–20	0.032	0.28	10
Graphite oxide/GCE	2.0	0.165–26.5	0.04	0.61	56
MWCNT–alumina coated silica/GCE	9.0	0.05–2	0.05	0.25	57
SWCNT–dicetyl phosphate film/GCE	6.5	0.1–20	0.04	0.36	59
Boron-doped diamond electrode	1.96	10–100	0.85	0.75	60
Carbon-coated nickel magnetic nanoparticle/GCE	3.0	7.8–110	2.3	0.52	61
Cadmium pentacyanonitrosylferrate/GCE	7.2	1.64–52.9	2.04	0.55	62
N-(3,4-Dihydroxyphenethyl)-3,5-dinitrobenzamide/carbon nanotube paste electrode	7.0	39.4–146.3	2.1	0.38	63

relatively low applied potential; these features show the promising future for applying the modified electrode into practical purpose. Additionally, the performance of rGO–PEDOT NT modified electrode is also comparable to other types of modified electrodes.[60–63]

3.5 The stability and reproducibility of the rGO–PEDOT NT modified electrode

The stability of a modified electrode is a key issue for developing effective sensors for practical purposes. Repetitive CV experiments were done to determine the stability of the rGO–PEDOT NT modified electrode in 0.1 M PBS (pH 7) for 100 continuous scan cycles, at a scan rate of 100 mV s^{-1}. After 100 scan cycles, the background current of the rGO–PEDOT NT modified electrode decreased to less than ~5%. Furthermore, the rGO–PEDOT NT modified electrode maintained more than 90% of its original electrochemical activity toward acetaminophen after one month of storage in air. This result implies that the rGO–PEDOT NT modified electrode shows high potential to be developed into a stable acetaminophen sensor for practical use. To investigate the reproducibility of the modified electrode, five sensors fabricated independently under the same conditions were examined in PBS and analyte solution. The results indicated that the modified electrodes showed excellent reproducibility. The relative standard deviation (RSD) was less than 2% (Fig. S1†).

3.6 Real sample analysis

The commercial pharmaceutical samples containing AP were determined by DPV using a 1standard addition method. The panadol tablet with a value of 500 mg AP (Panadol film coated caplets, GlaxoSmithKline, Taiwan) was used. The tablets were ground to powder, dissolved in pH 7 PBS, diluted and then spiked with different AP concentrations to produce final concentrations in the working range. A linear calibration plot is obtained for 0–15 μM spiked AP with a slope of 1.206 μA μM^{-1} and the recovery was obtained from 93.0 to 100.2% (Table S1†), considered to be acceptable recoveries. The results further substantiate that the rGO–PEDOT NT modified electrode could be applied for real sample detection.

4 Conclusion

A novel composite material combining PEDOT NTs and rGO sheets was developed and applied for the electrochemical detection of acetaminophen under neutral conditions. The SEM images reveal that the poor surface coverage of the 1D PEDOT NTs could be enhanced by blending the 2D rGO sheets. On the other hand, the PEDOT NTs could act as the conductive bridges to improve the electron conductivity between the isolated rGO regions. By combining the own unique advantages of the two materials, the obtained composite could exhibit high conductivity, which is beneficial for electrochemical application. From the CV measurements, the electrocatalytic ability of the GCE modified with rGO–PEDOT NT composite is much greater than that of the GCE only modified with rGO or PEDOT NTs; the catalytic current of the composite modified electrode also shows a good linear relationship with the concentration of acetaminophen up to 8.0 mM. The quantitative determination of acetaminophen by the rGO–PEDOT NT modified electrode was studied by DPV. A linear range of 1.0–35.0 μM and a detection limit of 0.4 μM were achieved in 0.1 M PBS (pH 7) at an applied potential of 0.38 V. The rGO–PEDOT NT modified electrode also exhibits excellent selectivity for acetaminophen against those common interferents and retains stable sensing ability after 100 cycles of CV scan or one month of storage. These features reveal that the proposed rGO–PEDOT NT based acetaminophen sensor shows high potential for applications for more practical purposes.

Acknowledgements

We thank the National Science Council of Taiwan and Academia Sinica, Taiwan, for the financial support. We thank Dr Rajeshkumar Mohanraman for technical assistance and helpful discussions.

Notes and references

1 R. N. Goyal, V. K. Gupta, M. Oyama and N. Bachheti, *Electrochem. Commun.*, 2005, **7**, 803–807.
2 R. T. Kachoosangi, G. G. Wildgoose and R. G. Compton, *Anal. Chim. Acta*, 2008, **618**, 54–60.
3 M. T. Olaleye and B. T. J. Rocha, *Exp. Toxicol. Pathol.*, 2008, **59**, 319–327.
4 Sirajuddin, A. R. Khaskheli, A. Shah, M. I. Bhanger, A. Niaz and S. Mahesar, *Spectrochim. Acta, Part A*, 2007, **68**, 747–751.
5 K. M. Alkharfy and R. F. Frye, *J. Chromatogr. B: Biomed. Sci. Appl.*, 2001, **753**, 303–308.
6 G. Burgot, F. Auffret and J. L. Burgot, *Anal. Chim. Acta*, 1997, **343**, 125–128.
7 M. Knochen, J. Giglio and B. F. Reis, *J. Pharm. Biomed. Anal.*, 2003, **33**, 191–197.
8 W. Ruengsitagoon, S. Liawruangrath and A. Townshend, *Talanta*, 2006, **69**, 976–983.
9 D. Yu, O. D. Renedo, B. Blankert, V. Sima, R. Sandulescu, J. Arcos and J.-M. Kauffmann, *Electroanalysis*, 2006, **18**, 1637–1642.
10 X. Kang, J. Wang, H. Wu, J. Liu, I. A. Aksay and Y. Lin, *Talanta*, 2010, **81**, 754–759.
11 M. S. M. Quintino, K. Araki, H. E. Toma and L. Angnes, *Electroanalysis*, 2002, **14**, 1629–1634.
12 X. Wang, L. Zhi and K. Müllen, *Nano Lett.*, 2008, **8**, 323–327.
13 S. R. C. Vivekchand, C. S. Rout, K. S. Subrahmanyam, A. Govindaraj and C. N. R. Rao, *J. Chem. Sci.*, 2008, **120**, 9–13.
14 Y. Wang, Y. Li, L. Tang, J. Lu and J. Li, *Electrochem. Commun.*, 2009, **11**, 889–892.
15 J. Li, S. Guo, Y. Zhai and E. Wang, *Electrochem. Commun.*, 2009, **11**, 1085–1088.
16 W. Hong, Y. Xu, G. Lu, C. Li and G. Shi, *Electrochem. Commun.*, 2008, **10**, 1555–1558.
17 O. Leenaerts, B. Partoens and F. M. Peeters, *Phys. Rev. B: Condens. Matter*, 2008, **77**, 125416.

18 P. K. Ang, W. Chen, A. T. S. Wee and P. L. Kian, *J. Am. Chem. Soc.*, 2008, **130**, 14392–14393.
19 Z. M. Ao, J. Yang, S. Li and Q. Jiang, *Chem. Phys. Lett.*, 2008, **461**, 276–279.
20 C. Shan, H. Yang, J. Song, D. Han, A. Ivaska and L. Niu, *Anal. Chem.*, 2009, **81**, 2378–2382.
21 D. J. Kang, H. Kang, K. H. Kim and B. J. Kim, *ACS Nano*, 2012, **6**, 7902–7909.
22 F. C. Krebs, S. A. Gevorgyan and J. Alstrup, *J. Mater. Chem.*, 2009, **19**, 5442–5451.
23 Q. B. Pei, G. Zuccarello, M. Ahlskog and O. Inganäs, *Polymer*, 1994, **35**, 1347–1351.
24 T. H. Lin and K. C. Ho, *Sol. Energy Mater. Sol. Cells*, 2006, **90**, 506–520.
25 C. Y. Lin, V. S. Vasantha and K. C. Ho, *Sens. Actuators, B*, 2009, **140**, 51–57.
26 H. Mao, X. C. Liu, D. M. Chao, L. L. Cui, Y. X. Li, W. J. Zhang and C. Wang, *J. Mater. Chem.*, 2010, **20**, 10277–10284.
27 S. Liu, J. Q. Tian, L. Wang, Y. L. Luo and X. P. Sun, *Analyst*, 2011, **136**, 4898–4902.
28 T. J. Li, C. Y. Lin, A. Balamurugan, C. W. Kung, J. Y. Wang, C. W. Hu, C. C. Wang, P. Y. Chen, R. Vittal and K. C. Ho, *Anal. Chim. Acta*, 2012, **737**, 55–63.
29 F. X. Jiang, R. R. Yue, Y. K. Du, J. K. Xu and P. Yang, *Biosens. Bioelectron.*, 2013, **44**, 127–131.
30 W. Y. Su and S. H. Cheng, *Electroanalysis*, 2010, **22**, 707–714.
31 Y. Li, Y. Feng and W. Feng, *Synth. Met.*, 2012, **162**, 781–787.
32 X. X. Bai, X. J. Hu, S. Y. Zhou, J. Yan, C. H. Sun, P. Chen and L. F. Li, *J. Mater. Chem.*, 2011, **21**, 7123–7129.
33 R. Trevisan, M. Döbbelin, P. P. Boix, E. M. Barea, R. Tena-Zaera, I. Mora-Seró and J. Bisquert, *Adv. Energy Mater.*, 2011, **1**, 781–784.
34 M. Kateb, V. Ahmadi and M. Mohseni, *Sol. Energy Mater. Sol. Cells*, 2013, **112**, 57–64.
35 S. Sotiropoulou, V. Gavalas, V. Vamvakaki and N. A. Chaniotakis, *Biosens. Bioelectron.*, 2003, **18**, 211–215.
36 J. Wang and Y. Lin, *TrAC, Trends Anal. Chem.*, 2008, **27**, 619–626.
37 Y. Shao, J. Wang, H. Wu, J. Liu, I. A. Aksay and Y. Lin, *Electroanalysis*, 2010, **22**, 1027–1036.
38 S. Ge, M. Yan, J. Lu, M. Zhang, F. Yu, J. Yu, X. Song and S. Yu, *Biosens. Bioelectron.*, 2012, **31**, 49–54.
39 F. Qu, H. Lu, M. Yang and C. Deng, *Biosens. Bioelectron.*, 2011, **26**, 4810–4814.
40 T. Yang, N. Zhou, Y. Zhang, W. Zhang, K. Jiao and G. Li, *Biosens. Bioelectron.*, 2009, **24**, 2165–2170.
41 Y. Xiao and M. L. Chang, *Electroanalysis*, 2008, **20**, 648–662.
42 R. Zhang and X. Wang, *Chem. Mater.*, 2007, **19**, 976–978.
43 J. J. Gooding, *Electrochim. Acta*, 2005, **50**, 3049–3060.
44 T. Y. Huang, J. H. Huang, H. Y. Wei, K. C. Ho and C. W. Chu, *Biosens. Bioelectron.*, 2013, **43**, 173–179.
45 W. S. Hummers and R. E. Offeman, *J. Am. Chem. Soc.*, 1958, **80**, 1339.
46 Y. Geng, S. J. Wang and J. K. Kim, *J. Colloid Interface Sci.*, 2009, **336**, 592–598.
47 D. A. Dikin, S. Stankovich, E. J. Zimney, R. D. Piner, G. H. B. Dommett, G. Evmenenko, S. Wu, S. Chen, C. Liu, S. T. Nguyen and R. S. Ruoff, *Nature*, 2007, **448**, 457–460.
48 M. J. McAllister, J. L. Li, D. H. Adamson, H. C. Schniepp, A. A. Abdala, J. Liu, M. Herrera-Alonso, D. L. Milius, R. Car, R. K. Prud'homme and I. A. Aksay, *Chem. Mater.*, 2007, **19**, 4396–4404.
49 E. Park, O. S. Kwon, S. J. Park, J. S. Lee, S. You and J. Jang, *J. Mater. Chem.*, 2012, **22**, 1521–1526.
50 S. S. Kumar, C. S. Kumar, J. Mathiyarasu and K. L. Phani, *Langmuir*, 2007, **23**, 3401–3408.
51 L. Zhang, H. Peng, P. A. Kilmartin, C. Soeller and J. Travas-Sejic, *Macromolecules*, 2008, **41**, 7671–7678.
52 S. Liu, J. Tian, L. Wang, Y. Luo, W. Lu and X. Sun, *Biosens. Bioelectron.*, 2011, **26**, 4491–4496.
53 A. J. Bard and L. R. Faulkner, *Electrochemical Methods*, Wiley, New York, 2nd edn, 2011, ch. 6, pp. 231–232.
54 Y. Ohnuki, H. Matsuda, T. Ohsaka and N. Oyama, *J. Electroanal. Chem.*, 1983, **158**, 55–67.
55 Q. Chu, L. Jiang, X. Tian and J. Ye, *Anal. Chim. Acta*, 2008, **606**, 246–251.
56 J. Song, J. Yang, J. Zeng, J. Tan and L. Zhang, *Sens. Actuators, B*, 2011, **155**, 220–225.
57 T.-L. Lu and Y.-C. Tsai, *Sens. Actuators, B*, 2011, **153**, 439–444.
58 X. Chen, J. Zhu, Q. Xi and W. Yang, *Sens. Actuators, B*, 2012, **161**, 648–654.
59 D. Sun and H. Zhang, *Microchim. Acta*, 2007, **158**, 131–136.
60 C. Radovan, C. Cofan and D. Cinghita, *Electroanalysis*, 2008, **20**, 1346–1353.
61 S.-F. Wang, F. Xie and R.-F. Hu, *Sens. Actuators, B*, 2007, **123**, 495–500.
62 H. Razmi and M. Harasi, *J. Iran. Chem. Soc.*, 2008, **5**, 296–305.
63 A. A. Ensafi, H. Karimi-Maleh and S. Mallakpour, *Electroanalysis*, 2012, **24**, 666–675.